Natural Hazards (2026) 122:353
https://doi.org/10.1007/s11069-025-07751-w

ORIGINAL PAPER

Predicting hydrological drought at global scale: an analysis of the CEMS seasonal forecasts

Vanesa García-Gamero[1] · Carmelo Cammalleri[1] · Alessandro Ceppi[1] · Christel Prudhomme[2] · Arthur Ramos[2] · Juan Camilo Acosta Navarro[3] · Andrea Toreti[3]

Received: 28 July 2025 / Accepted: 3 December 2025 / Published online: 1 April 2026

Abstract
Drought is among the most severe hydro-meteorological events, and it is expected to become even more critical and recurrent in multiple regions worldwide. The availability of hydrological information months ahead is crucial for developing effective early warning strategies, which often remain focused on meteorological drought, and to support effective adaptation programs and enhanced preparedness. The Copernicus Emergency Management System (CEMS) provides seasonal ensemble forecasts of river discharge based on the LISFLOOD hydrological model simulations, which are driven by seasonal meteorological ensemble forecasts from the seasonal forecast system version 5 (SEAS5) by the European Centre for Medium-Range Weather Forecasts (ECMWF). In this study, we evaluate the performance of these forecasts in detecting hydrological drought in the period 1991–2022 using the ECMWF reanalysis ERA5 as a proxy for the observational reference. The main results show that the skill of the ensemble mean of the Standardized Streamflow Index (SSI) is high at both 1- and 3-month time horizons; lower-skill forecasts (but still informative) can be achieved up to 6 months ahead. The forecast always outperforms trivial ones done by using the latest available state of the reanalysis, with the highest added value, on average, in the Northern Hemisphere. Seasonality in average river discharge is highlighted as one of the main drivers of the differences in skill between seasons. Additionally, the dominant role of inter-annual variability in initial conditions (soil moisture) and meteorological forcings (precipitation) on forecast skill is observed in summer and spring–summer for the former, and in winter and autumn–winter for the latter. Besides the high skill observed with the ensemble mean, the signal-to-noise ratio (SNR) of the ensemble forecast is identified as key metric to operationally assess and communicate forecast reliability.

Keywords Standardized streamflow index · LISFLOOD · Drought forecasts · Signal-to-noise ratio · Ensembles · Hydro-meteorological forecasts · Dry spells

Extended author information available on the last page of the article

1 Introduction

Drought is considered one of the most severe weather-related natural hazards, mainly due to its ability to manifest everywhere in the globe, and the tendency to affect large areas for an extended period (UNDRR, 2022). Recent catastrophic events with well-documented impacts were observed in all the continents, including the 2012 US drought (Hoerling et al. 2014), the 2003 and 2018 European droughts (Rebetez et al. 2006; Toreti et al. 2019), the 'millennium' drought in Australia (Van Dijk et al. 2013), the 'day zero' drought in Cape Town (Sousa et al. 2018), the 2019–2022 multi-annual drought in Central South America (Arias et al. 2024), the 2016–2018 southern India drought (Mishra et al. 2021) and the events in the late 2000s in Ethiopia (Viste et al. 2013).

Drought is primarily triggered by the lack of precipitation for an extended period of time. This precipitation deficit may reverberate through the water cycle, causing a reduction in soil moisture, lower river discharge and further affecting groundwater recharge (Tallaksen and van Lanen, 2023). A reduction in river discharge may lead to what is here called hydrological (or streamflow) drought. Analysis on hydrological droughts adds valuable information to meteorological drought, as many economic sectors and ecosystems are affected by these events both directly and indirectly (Stahl et al. 2016; Lackstrom et al. 2017).

As for proactive drought management, forecasting is valuable to enabling effective and timely actions. However, due to the complex spatiotemporal evolution, drought events are usually difficult to predict and their impacts difficult to robustly identify and quantify. Drought management has traditionally relied on crisis response or reactive approach, but managing effectively drought risk requires a transition to perspective and proactive approaches, aiming to prevent or mitigate its impacts and risks well in advance (Biella et al. 2025). Define and design preparedness measures, such as early actions and long-term planning decisions, are subject to, among other things, the provision of reliable and usefulness sub-seasonal to seasonal (S2S) forecast to support decision-making (UNDRR, 2021).

Whilst several drought early warning systems exist at regional and global scale, many of which include forecasting tools, they tend to primarily provide information on the meteorological component of drought (Tallaksen and van Lanen, 2023). Meteorological drought indices can be directly derived from these forecasts, as in the case of the Unusually Wet and Dry Conditions Index, currently implemented in the Copernicus Global Drought Observatory (GDO, https://drought.emergency.copernicus.eu/tumbo/gdo/map/, accessed on 1st July 2025) and based on the Standardized Precipitation Index (SPI) (Mckee et al. 1993; Lavaysse et al. 2020). However, there is currently no hydrological drought forecast product that covers operationally the entire globe.

S2S predictions of drought-related variables can be achieved through statistical, dynamical, or hybrid methods, also leveraging artificial intelligence (AI) (Hao et al. 2018). Within the dynamical (model-based) approach, ensemble forecasting has become well established in the field of hydrometeorological forecasting because it quantifies the uncertainty by generating a range of possible future streamflow outcomes (Troin et al. 2021).

Hydrometeorological forecasts based on hydrological models forced with short and long term weather forecasts exploit the predictability in the meteorological forcings as well as the effects of initial conditions of the hydrological variables. Several authors have pointed to higher predictability of hydrological drought (based on hydrometeorological forecasts) compared to meteorological drought (Yuan et al. 2013; Zhang et al. 2017; Sutanto et al.

2020). This represents a sound alternative to the commonly used Ensemble Streamflow Prediction (ESP) method (Day 1985), in which predictability mainly stems from the memory effect and quickly decays after one month (Wood et al. 2015).

Predictability of hydrological quantities has been widely investigated in the recent past. Generally, the key role of initial hydrological conditions has been repeatedly stressed (e.g., Wood and Lettenmaier 2008). Shukla et al. (2013), using the variable infiltration capacity (VIC) model, quantified the effects of both the initial hydrological conditions and the seasonal forecast skill. They observed regional and time dependent differences in the relative contributions of initial conditions and forecast skill. For instance, more prominent role of initial conditions was found in arid and snow-dominated regions of the Northern Hemisphere in January and October, while forecast skill was estimated to be more important in the equatorial and monsoon region along the year. Similarly, Yossef et al. (2013) highlighted the important role of the initial state of surface and groundwater in forecasting hydrological variables for large basins. In a recent assessment of seasonal river flow forecast across catchments in the Republic of Korea, Lee et al. (2024) found higher forecast skill at 1 month lead time, outperforming the ESP, particularly during the wet season, highlighting how precipitation is the most important variable affecting predictability.

The effects of initial conditions on predictability are strongly linked to memory and persistence (i.e., autocorrelation) in hydrological variables. Thober et al. (2015) showed how autocorrelation can be used to indicate forecast dependence on initial conditions, while Nicolai-Shaw et al. (2016) successfully used antecedent soil moisture or discharge data to represent persistence.

The quality of forecasts is also influenced by the pre-processing procedures deployed to reduce biases. Shi et al. (2008) investigated how hydrological model calibration and bias correction contribute to reducing forecast errors, while Thober et al. (2015) highlighted the role of standardization of the hydrological forecast values, showing how different procedures can lead to drastically different results. Thober et al. (2015) highlighted that transforming the ensemble mean of a soil moisture forecast into a standardized index is more efficient for forecasting than the mean of individual standardized indices computed from each ensemble member. The use of self-consistent baseline data for standardization is also a key factor in ensuring consistency between forecast and historical data (Shao and Li 2013).

Recently, Acosta Navarro and Toreti (2023) highlighted how the SNR of a multi-system ensemble of predictions can be used as a proxy of forecast accuracy for temperature and precipitation during boreal summer months. Albeit significantly improved in the past years (Merryfield et al. 2020), the forecast skills for temperature and precipitation at seasonal scale are still low for meteorological drought predictions based on climate models (Aghakouchak et al. 2022).

Currently, global-scale seasonal forecasts of hydrological quantities are operationally generated by the Global Flood Awareness System (GloFAS, https://global-flood.emergency.copernicus.eu/, accessed on 1st July 2025) as part of CEMS (Emerton et al. 2018). The Glo FAS system provides an outlook on river flood conditions at S2S scale based on LISFLOOD model simulations forced with predictions from the ECMWF SEAS5 (Johnson et al. 2019). Despite the richness of this forecast dataset, its value for drought forecasting at global scale has not been fully investigated yet, while a similar dataset over Europe has shown promising results (Sutanto et al., 2021).

The goal of this study is to exploit CEMS seasonal forecasts for hydrological drought forecasting, particularly the quantification of forecast skill at different temporal scales across the globe, and the detection of the main sources of predictability. The analyses are performed on forecasts for past years (1991–2022, reforecasts), which are compared against simulations forced with ECMWF ERA5 (Hersbach et al. 2020), with the latter used as a proxy of the ground truth. The outcomes of this evaluation will support the operational implementation of a new seasonal hydrological forecast indicator to enhance the CEMS portfolio of drought indicators.

2 Materials and methods

2.1 The CEMS GloFAS datasets

The hydrological datasets produced as part of CEMS GloFAS are based on the LISFLOOD rainfall-runoff model (De Roo et al. 2000; Van der Knijff et al. 2010). LISFLOOD is an open source (https://ec-jrc.github.io/lisflood, accessed on 1st July 2025) spatially distributed physically based model simulating all the main hydrological processes at grid cell (evapotranspiration, infiltration, snow formation, etc.), as well as the routing of runoff through the river network. In GloFAS v.4.0, model outputs are generated on regular lat/lon grids at 0.05° spatial resolution, daily time steps, and with quasi-global coverage (from 90º N to − 60° S). All the GloFAS data are distributed via the CEMS Early Warning Data Store (EWDS, https://ewds.climate.copernicus.eu, accessed on 1st July 2025).

Two datasets are used in this study, the first one is obtained by forcing LISFLOOD with ERA5 (Grimaldi et al. 2022). This dataset (hereafter G-E) is updated in near-real time (with a few days of delay), and it is here used as reference to evaluate the performance of the seasonal forecasts. Obtaining an observation-based reference dataset for validating hydrological drought forecast at global scale is challenging, as observational networks are limited.

LISFLOOD has been calibrated and validated on a global scale over more than 1,800 flow gauges, similarly to what described in Harrigan et al. (2020). This model has been previously used in drought monitoring, forecasting, and projection studies with good results (e.g., Sepulcre-Canto et al. 2012; Forzieri et al. 2014; Sutanto et al. 2024) and has been calibrated and validated in many experiments. Cammalleri et al. (2020) performed a validation exercise focusing on drought, showing overall good model performance, characterized by high efficiency and a small negative percentage bias for annual minima and total deficit during the period 1990–2016 at 437 stations distributed across Europe.

The second dataset here used is the ensemble forecast produced for past years (reforecast or hindcast) obtained by forcing LISFLOOD with the ECMWF SEAS5 seasonal reforecasts (Grimaldi et al. 2023). This dataset (G-S hereafter) includes 25 members (51 from 2017), and it is generated once a month for a temporal horizon up to 7 months. A flowchart summarizing the methodology, including the use of G-E and G-S as input data, is provided in Fig. 1. For both datasets, river discharge, Q ($m^3\ s^{-1}$), is analyzed from 1991 to 2022 as a key variable representative of hydrological droughts (WMO and GWP, 2016). River discharge is influenced by surface conditions, subsurface processes as well as meteorological factors.

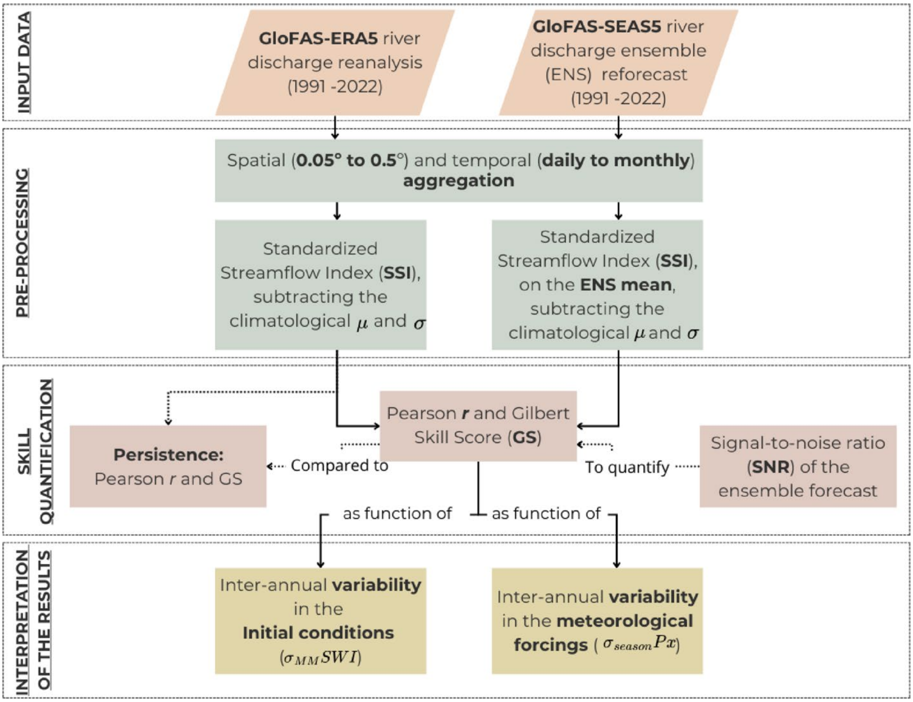

Fig. 1 GloFAS-ERA5 reanalysis data and GloFAS-SEAS5 seasonal ensemble reforecast are the two datasets used in this study. For both datasets, river discharge is analyzed from 1991 to 2022. The datasets are initially aggregated spatially and temporally, then converted into standardized anomalies (SSI) by subtracting the climatological mean, μ, and dividing the result by the standard deviation, σ. The metrics used to assess skill are: the Pearson correlation coefficient (*r*) and the Gilbert Skill (GS) Score. Additionally, forecast performance is compared to results from persistence analysis, using the latest available reanalysis as antecedent condition. The signal-to-noise ratio (SNR) is also calculated as a complementary metric to quantify forecast skill operationally. Finally, the forecast skill results are interpreted based on the interannual variability in both initial conditions and meteorological forcings

2.2 Data pre-processing

The G-E and G-S datasets are characterized by relatively high spatial (0.05°) and temporal (daily) resolutions. At seasonal and global scales, hydrological drought forecasts aim at identifying large-scale patterns of areas potentially impacted by drought and they are not meant for local scale or short-term applications. Global-scale forecast and modelling frameworks complement, when they exist, detailed local forecasts and modelling systems (with homogeneous larger-scale evaluations and often longer lead times) based on higher-resolution data and enhanced knowledge of catchment processes. Those local systems usually hold the mandate to issue warnings, and support emergency action on the ground (Dasgupta et al. 2025).

The two datasets are preliminarily aggregated both spatially and temporally to obtain data in line with the usual characteristics of drought seasonal forecasts (see the “Pre-Processing” step in the methodological flowchart, Fig. 1). As an example, the current drought forecast product in GDO, based on a multi-system ensemble of SPI, is generated at a spatial resolution of 1° (European Commission 2025), while the raw SEAS5 meteorological forcings have a resolution of about 36 km (Johnson et al. 2019).

Spatially, the data are aggregated at 0.5° resolution following a weighted average of the Q values within each coarse resolution grid cell (with weight proportional to the drainage area). Commonly, river network upscaling is performed by finding the fine-resolution cell with the maximum drainage area (Arora and Harrison 2007); here, this procedure is generalized by accounting for the fact that the pixel with the largest drainage area may not necessarily be the only one characterizing the coarse resolution, although major rivers should have higher weight in the aggregation when compared to smaller tributaries. At the temporal level, data are aggregated into monthly values by taking a simple average of daily values. It is worth noting that there are no gaps in the simulated time series. Since drought indices are usually computed on multi-month accumulations (as described later in this section), the monthly aggregation does not affect the results.

The aggregated datasets are converted into standardized anomalies using the z-score approach in the reference period 1991–2020 (see also the "Pre-Processing" step in Fig. 1, where the standardization procedure is illustrated). This period corresponds to the standard climatological reference for normal (WMO, 2017), and it is used for both G-E and G-S. In the case of forecasts, we first computed the ensemble mean, i.e., the average of the forecast values of the ensemble members, and then performed the standardization as suggested by Thober et al. (2015).

The standardized quantities, namely Standardized Streamflow Index (SSI), are computed on three most used accumulation periods: a month, 3 months, and 6 months. This makes possible to capturing different stages of hydrological drought development, from short-term up to the next months ahead. In the case of G-S, the forecasts used are the ones initialized at the beginning of the accumulation period, always including the forecast data only. For instance, SSI-3 (3-month accumulation) for the month of January includes the river discharge for January, February, and March from the forecast issued on January 1st. Even if the LISFLOOD model simulates Q across the entire quasi-global domain, data over some grid cells are not reliable for drought analyses due to the discharge being too low (often close to 0) most of the time. If we assume that droughts occur when the SSI is lower than −1, these conditions are unrealizable when $\mu - \sigma \leq 0$. Grid cells where this condition occurs on 6-month accumulated Q, derived from the G-E dataset, for more than 3 months are masked in all the analyses we performed. The resulting static mask excluded approximately 23% of the previously valid grid cells, including most of the deserts (hot and cold), as well as regions with ephemeral rivers with predominant no-flow conditions.

2.3 Evaluation strategy

2.3.1 Assessment of seasonal forecast skill

The skill of the seasonal hydrological forecasts (G-S) is evaluated by using the standardized anomalies (SSI) derived from the G-E dataset as a reference. Using SSI removes the seasonality of the data, making correlation a robust metric for evaluating forecast performance. Therefore, two main metrics are computed to quantify the skill: the Pearson correlation coefficient (r) and the Gilbert Skill (GS) Score (Jolliffe and Stephenson 2003; Wilks 2020) (see the "Skill Quantification" step in Fig. 1 for a schematic overview of the assessment process). While r characterizes the correlation between the two standardized datasets over the full range of data, the GS quantifies the skill in reproducing extremes, here defined as negative anomalies below −0.67 (corresponding to the 25-th percentile in the standard normal distribution). Both metrics are computed on the ensemble mean of the G-S dataset.

Different temporal windows are considered in the analysis: full year (Y, January–December); boreal summer (JJA, June–August), boreal winter (DJF, December–February), spring-boreal summer (MAM-JJA, March–August), autumn- boreal winter (SON-DJF, September–February). Hereafter, we will use the terms summer and winter with the implicit assumption they refer to the Northern Hemisphere.

The full year, here, translates in twelve SSI-1, -3, and -6. Summer is just one SSI-3 for the period JJA, and the equivalent for winter is a single SSI-3 for the period DJF. Concerning spring–summer (MAM-JJA), there are four SSI-3 (generated in March, April, May, and June) and one SSI-6 (generated in March), the same holds true for autumn–winter (SON-DJF), with four SSI-3 (generated in September, October, November, and December) and one SSI-6 (generated in September).

2.3.2 Analysis of persistence

Since initial conditions and persistence have proven to be key factors in the predictability of hydrological quantities, the forecast performance is compared against the results obtained by using the latest available reanalysis as antecedent condition (see the "Persistence" branch within the "Skill Quantification" step in Fig. 1). This analysis aims at assessing the added value of the forecast over the simplest approach based on persistence, assuming the latter being the best dataset easily available for decision makers in the absence of any forecast information. To this aim, we computed the same skill metrics used in the previous analyses (r and GS) but using the SSI-1 of the month preceding the forecast from the G-E dataset. For example, as for summer, the forecast skill for SSI-3_{JJA} (June–August) computed between G-S and G-E is compared with the skill obtained using SSI-1_{May} from G-E (which represents the latest available reanalysis data before the forecast period), and SSI-3_{JJA} also from G-E (this last part remains the same in both cases).

2.3.3 Effect of inter-annual variability and seasonality

The results of the forecast skill analysis are evaluated as a function of the inter-annual variability in both the initial conditions and the meteorological forcings (see the "Interpretation of the Results" step in Fig. 1, which summarizes these relationships). In this study, the inter-annual standard deviation of soil moisture conditions (quantified by the Soil Wetness Index, SWI) in the last antecedent month is used as a proxy for the variability in the initial condition (e.g., σ_{May} of SWI for summer, JJA), while the inter-annual standard deviation of ERA5 precipitation (P) during the forecast period is used to quantify the variability in the forcing (e.g., σ_{JJA} of P-3 for summer). Following Bierkens and Van Beek (2009) in their skill assessment of river discharge seasonal forecasts across Europe, higher inter-annual variability in the parameters used for the initial conditions and slow response of the system to changes in meteorological forcings are expected to have affect the skill. Therefore, a good representation of the initial conditions becomes important for the river discharge forecast in the months ahead. Skill is also influenced by the inter-annual variability of precipitation, as lower values make forecasting easier and the skill higher.

Moreover, seasonality in the hydrological variables can also be a factor in the overall skill, especially in explaining differences observed between opposite periods (i.e., summer and winter). The intra-annual variability in river discharge is quantified as $\Delta_{\mathrm{JJA-DJF}} = (\mu_{\mathrm{JJA}} - \mu_{\mathrm{DJF}})/\mu_{\mathrm{Y}}$, where μ_{JJA} and μ_{DJF} are the average river discharge during summer and winter months, respectively, and μ_{Y} is the average annual river discharge during the study period. This quantity is positive when Q is higher during the summer months, negative when Q is higher during the winter months, and close to zero in areas with limited seasonality. $\Delta_{\text{JJA-DJF}}$ is here used as a proxy variable of river seasonality to investigate the difference in forecast skill between seasons.

2.3.4 Ensemble spread

The SNR of the ensemble is evaluated to provide information about the reliability of the hydrological forecasts (see the "Signal-to-noise ratio (SNR)" branch within the "Skill Quantification" step in Fig. 1). Although the ensemble mean is expected to be the best estimate of the future conditions, the SNR provides relevant information that can be used to assess the reliability of the forecast in near-real-time (Acosta-Navarro and Toreti, 2023), given that skill is usually estimated once and assuming it will not change over time. Following Acosta Navarro and Toreti (2023), $SNR = \frac{|\mu_e|}{\sigma_e}$, where $|\mu_e|$ is the absolute value of the ensemble mean and σ_e is the ensemble standard deviation, computed across ensemble members for every summer (JJA), spring–summer (MAM-JJA), winter (DJF), and autumn–winter (SON-DJF) 3 and 6 months ahead for each year. To check the agreement of SNR with the skill metrics, the yearly SNR values were averaged over the study period from 1991 to 2022.

To better evaluate the role of SNR in providing relevant information to forecast reliability, the density distribution histogram of the mean absolute difference (MAD) between the ensemble mean forecast and reanalysis $|SSIx_{G-S} - SSIx_{G-E}|$ is computed for 3- and 6-month time horizons across different periods, and compared with the SNR values for each corresponding date (and different thresholds of SNR). As the focus of this study is on the prediction of dry extremes, all these analyses were limited to dry conditions in the reanalysis (ERA5, defined as negative anomalies below −0.67).

3 Results

3.1 Assessment of hydrological drought seasonal forecast

Results on the estimated forecast skill across the quasi-global domain are first reported in terms of Pearson *r*. Overall, the forecasts of hydrological drought conditions are skillful when data for the full year are considered, with higher Pearson *r*, on average, for 1 (SSI-1) and 3 (SSI-3) and 6 (SSI-6) months forecasts (Fig. 2b–d). Results for the three accumulation periods are similar in terms of spatial patterns (Fig. 2a; refer to Fig. S1 in the supplementary material for the spatial patterns corresponding to SSI-1 and SSI-3). As expected, the forecast performance slightly deteriorates with the increased time horizon.

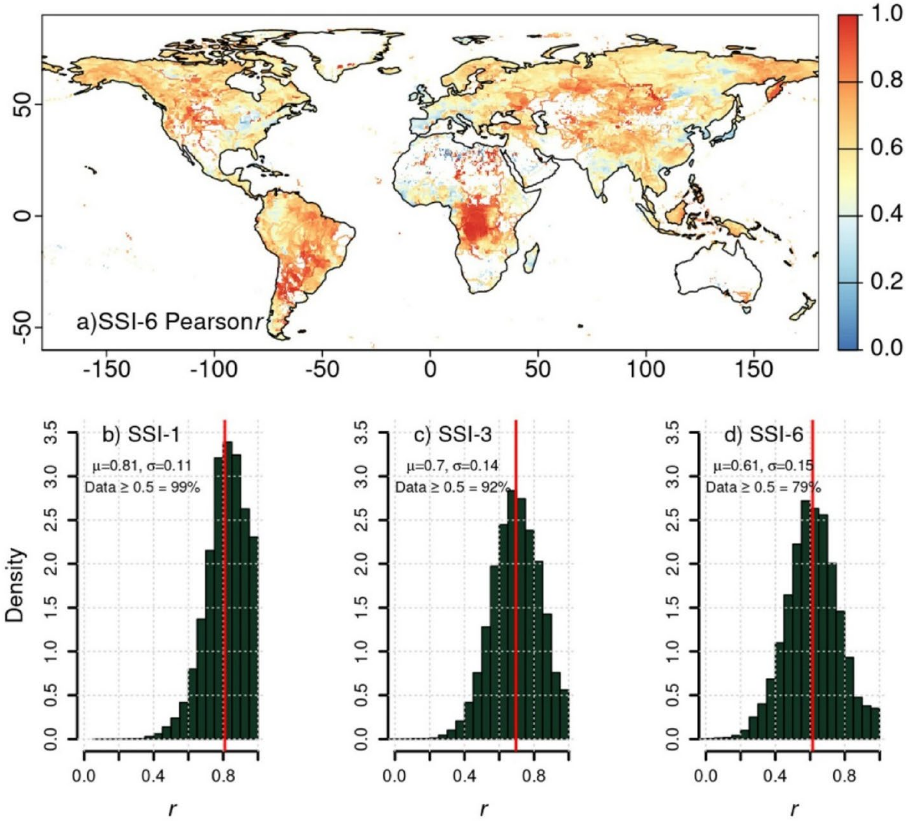

Fig. 2 Analysis of predictability on the entire annual dataset using the Pearson r metric. **a** Spatial distribution of the ensemble-mean Pearson r for a temporal horizon of 6 months (SSI-6) for the full year. Lower panel: the histograms show the mean (red line), μ, standard deviation, σ, and the percentage of cells with significant r values for **b** SSI-1, **c** SSI-3, and **d** SSI-6. As no negative correlation values have been estimated, the Pearson r is here shown from 0 to 1

To provide a concise representation of the forecast performance, a threshold $r=0.5$ is chosen to distinguish skillful forecasts. For SSI-1, skill is found to be almost globally above the chosen threshold (99% of the cells$\geq$0.5). There is a tendency of decreasing skill at longer forecast range for both SSI-3 and SSI-6. However, skillful forecasts are still found for most of the domain (92% and 79% of the cells being$\geq$0.5, respectively).

The spatial patterns in GS resemble those observed for Pearson r, as exemplified by Fig. 3 for SSI-6 for the full year, with skillful forecast of extremes denoted by positive value. Overall, an average GS Score equal to 0.30 ± 0.15 is obtained for SSI-6 (see Fig. S2 in the supplementary material for the spatial patterns corresponding to SSI-1 and SSI-3). Due to the high similarity between the estimated r and GS, successive analyses will mostly focus on Pearson r, except where differences in the results are relevant.

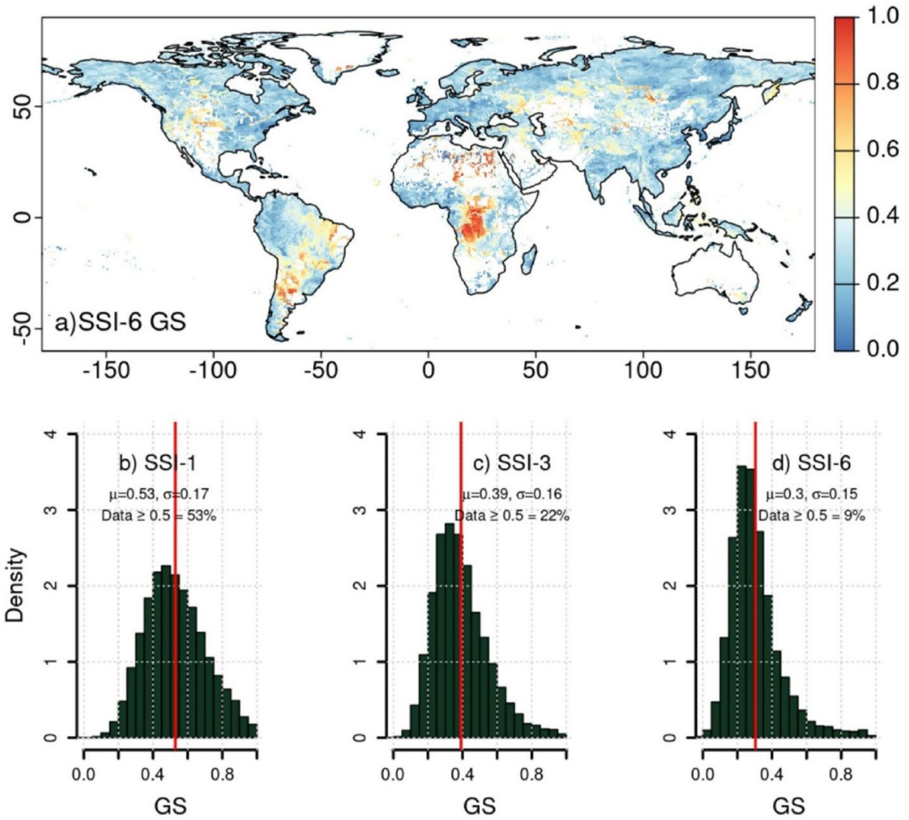

Fig. 3 Analysis of predictability on the entire annual dataset using the Gilbert Skill (GS) Score. **a** Spatial distribution of the ensemble-mean GS for a temporal horizon of 6 months (SSI-6) for the full year. Lower panel: the histograms show the mean (red line), μ, standard deviation, σ, and the percentage of cells with significant GS values for **b** SSI-1, **c** SSI-3, and **d** SSI-6. As no negative values have been estimated, the GS is here shown from 0 to 1

3.2 Seasonality in hydrological drought forecast skill

Predictability is neither stationary in space nor in time, thus, additional analysis to evaluate the skill in each season is needed to get a better overview. Figure 4 (panels a and b) shows the estimated skill for SSI-3 in summer (JJA) and winter (DJF), respectively, while Fig. 4c shows the difference in skill between the two seasons (JJA – DJF). These results highlight a concentration of positive values (higher skill in JJA) in the Southern Hemisphere, Europe and the Middle East, and some regions of North America. Negative values, i.e. higher skill in DJF, are mostly estimated over the Asian continent and around the Sahel in Africa. This difference can be partially related to river discharge seasonality $\Delta_{JJA\text{-}DJF}$. Indeed, we found that overall, the skill is higher when the average river discharge is lower (Fig. 4d). This dependency is stronger for summer–winter (JJA-DJF) than for spring–summer and autumn–winter (MAM-JJA – SON-DJF) (see Figs. S3 and S4 in the supplementary material for SSI-3 and SSI-6 in spring–summer, MAM-JJA, and autumn–winter, SON-DJF).

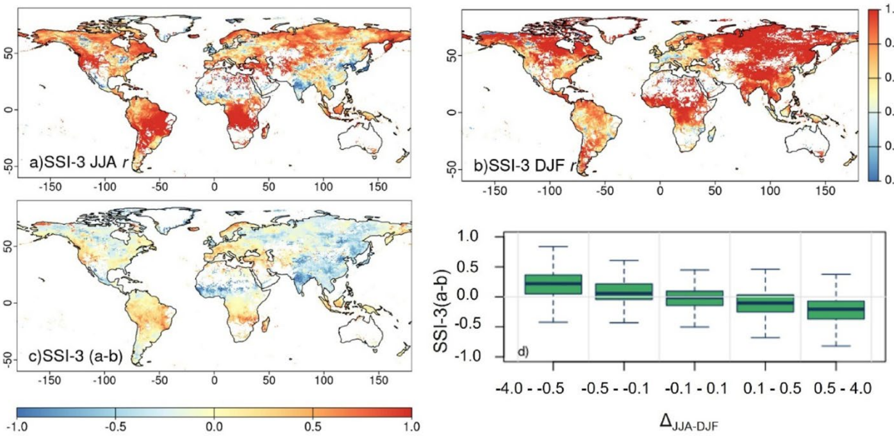

Fig. 4 Spatial distribution of the Pearson r for a temporal horizon of 3 months (SSI-3) at: **a** June–August (JJA) and **b** December-February (DJF). Panel **c** shows the differences in r between the two seasons (**a**, **b**), while panel **d** reports the boxplot of the seasonal forecast skill differences SSI-3 (**a**-**b**) as a function of river discharge seasonality, $\Delta_{\text{JJA}-\text{DJF}}$. The lower and upper ends of the box represent the first and third quartiles, respectively, and the whiskers extend to the most extreme value within 1.5 IQR (interquartile range)

3.3 Forecast skill over persistence

Figure 5 shows the added value of forecast over persistence expressed as skill difference ($\overline{r_{forecast} - r_{persistence}}$) averaged on 10º latitude bands for the three studied time horizons (1-, 3-, and 6-months ahead). Overall, the seasonal forecast outperforms the trivial forecast based on persistence in all cases (i.e., positive differences). There are similar patterns in the added value across the domain for the three accumulation periods, with larger positive differences at higher latitudes for SSI-6 during the autumn–winter (SON-DJF) season (Fig. 5a-c). Generally, there is a marked North–South difference in spring–summer (MAM-JJA), with an added forecast value up to 0.5 in the northernmost latitudes for SSI-3 and SSI-6 (Fig. 5d–f). However, particularly around the Tropic of Cancer, the added value is limited for both SSI-3 and SSI-6 in MAM-JJA (Fig. 5e, f; see Fig. S5 in the supplementary material for winter (DJF) and summer (JJA)). The reader is referred to Figs. S6 and S7, in the supplementary material, for the spatial patterns of the difference between r_{forecast} and $r_{\text{persistence}}$ in all the studied seasons and time horizons.

3.4 Main drivers of hydrological drought forecast predictability

To better understand the main drivers of hydrological drought predictability, apart from the river discharge seasonality previously reported, we investigate two potential sources: the initial conditions and the meteorological forcing (Figs. 6 and 7, respectively). Except for SSI-3 in winter (DJF), the results reveal a dependency of the estimated Pearson r on the inter-annual variability of initial conditions, with a slight tendency of increasing mean skill associated with higher standard deviation of the SWI, albeit a large spread is observed in these results.

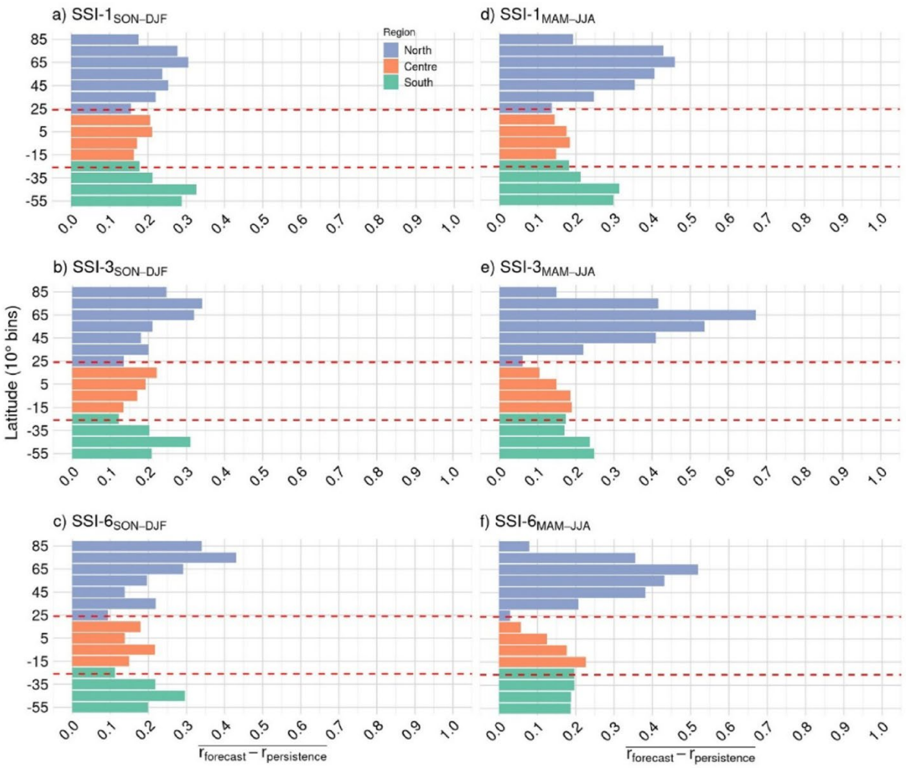

Fig. 5 Average difference in Person r between forecast and persistence at 10º latitude bands, in autumn–winter (SON-DJF) for **a** SSI-1, **b** SSI-3, **c** SSI-6, and in spring–summer (MAM-JJA) for **d** SSI-1, **e** SSI-3, **f** SSI-6. We set the subdivision of the World around the Tropics, with North defined from 90° to 25°, South from −25° to −60°, and Centre roughly as the Tropics from 25° to −25°. These regions follow the GloFAS v.4.0 model coverage from 90ºN up to 60ºS

Conversely, the results point toward an inverse relationship of the forecast skill with the inter-annual standard deviation of the precipitation during the forecast period, as a clear tendency to decreasing mean skill with increasing precipitation variability is observed in winter (DJF) and autumn–winter (SON-DJF) for both SSI-3 and SSI-6 (Fig. 7a–c). This behavior is not observed in spring–summer (MAM-JJA) for SSI 3 and 6 (Fig. 7e–f), pointing to a different response to precipitation variability in spring.

3.5 Relationship between signal-to-noise ratio and forecast skill

Figure 8 (a and d) shows the spatial patterns of the time-averaged SNR for summer (JJA) and winter (DJF), as well as the corresponding scatterplots of the relationship of SNR with the Pearson r (Fig. 8 b and e) and GS (Fig. 8 c and f). Overall, there is a positive relationship between both skill metrics and SNR, with the spatial patterns of the SNR closely resembling those of the Pearson r (Fig. 4a and b). However, there are regions showing large differences between the two metrics, e.g., in Northern and Eastern Canada or Russia in summer (JJA).

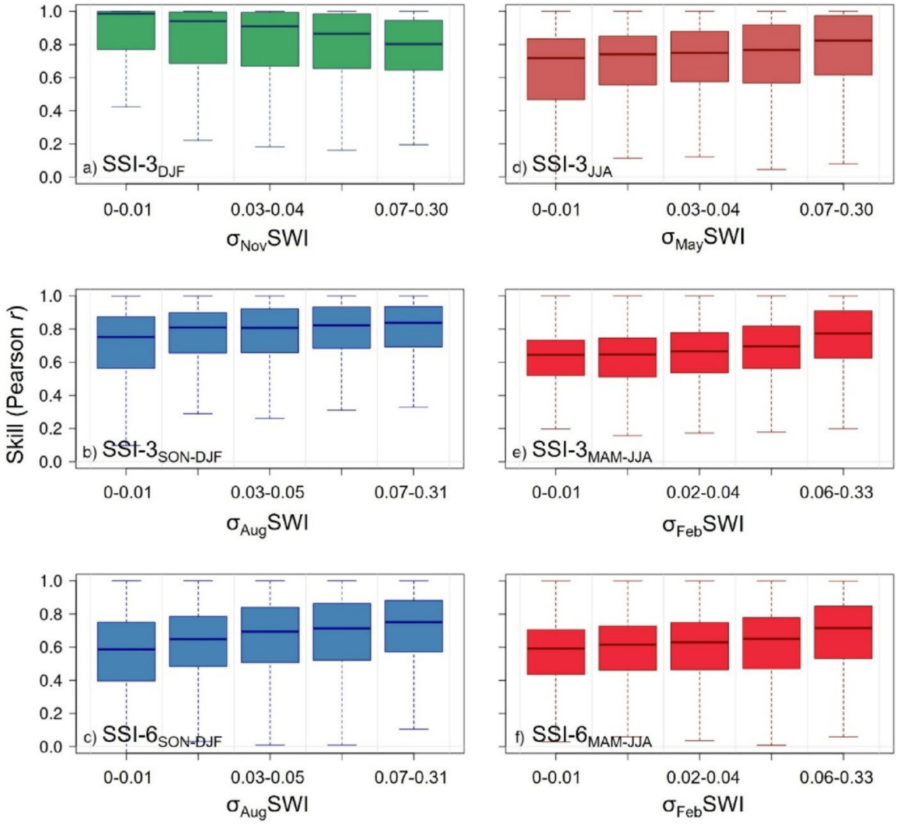

Fig. 6 Boxplot of Skill (Pearson *r*) for **a** winter (DJF) SSI-3, **b** autumn–winter (SON-DJF) SSI-3, and **c** SSI-6, for **d** summer (JJA) SSI-3, and **e** spring–summer (MAM-JJA) SSI-3, and **f** SSI-6 for inter-annual variability of the previous month Soil Wetness Index (σ_{MM} SWI). The range of Pearson *r* is here set as 0–1 since no negative correlation values have been estimated. Boxplot colors are used solely to distinguish the season under study

In winter (DJF), some of these regions are in the East of the US, the Amazon basin, and the East and South of China.

These discrepancies are also exemplified by the large scatter in the boxplot around the mean behavior. Indeed, in both the relationships between Pearson *r* (SSI-3*r*) and GS (SSI-3*GS*) with SNR (Fig. 8b and -c for summer, JJA; Fig. 8e and -f for winter, DJF) the boxplot are characterized by a large variability, which is only limited for SSI-3*r* at high SNR values (see Figs. S8 and S9 in the supplementary material for the other seasons and time horizon). This result is associated with an average Pearson *r* that tends to saturate at higher SNR values, introducing a nonlinearity in the relationship. In contrast, the relationships between GS and SNR are more linear, but also characterized by a greater variability, as indicated by the larger interquartile ranges and whiskers, particularly at SNR values > 2.

From the results shown in Fig. 8, it is possible to deduce a potential strategy for characterizing the reliability of the hydrological drought forecast in near real time using SNR. Normally, higher average skill hydrological drought forecasts are associated with SNR > 2

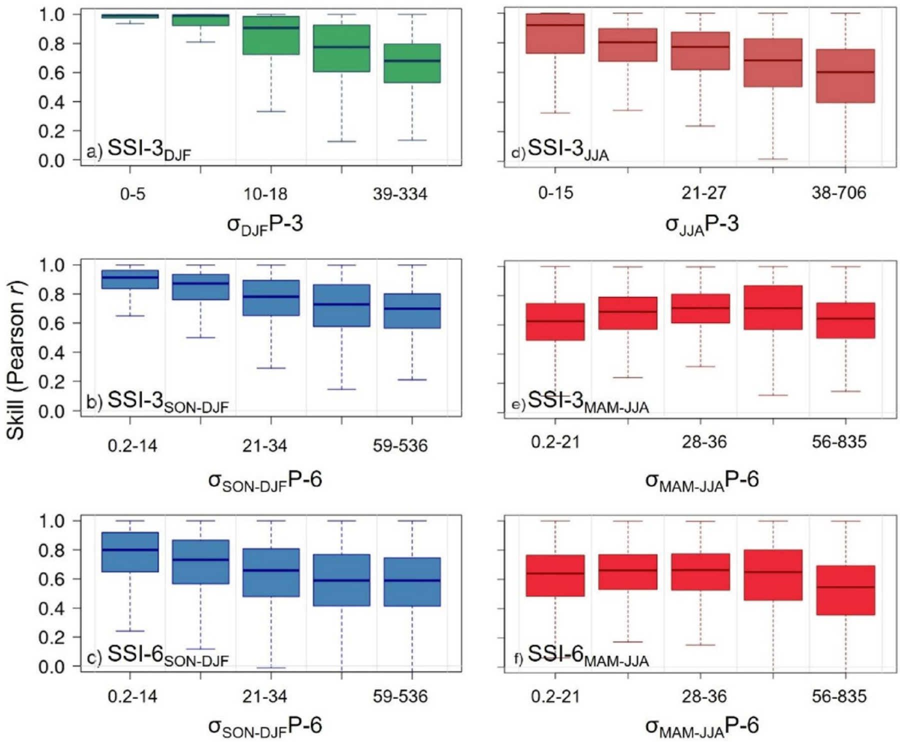

Fig. 7 Boxplot of Skill (Pearson *r*) for **a** winter (DJF) SSI-3, **b** autumn–winter (SON-DJF) SSI-3, and **c** SSI-6, for **d** summer (JJA) SSI-3, and **e** spring–summer (MAM-JJA) SSI-3, and **f** SSI-6 for the interannual variability of the precipitation during the forecast period (σseason Px). The range of Pearson *r* is here set as 0–1 since no negative correlation values have been estimated. Boxplot colors are used solely to distinguish the season under study

compared to the values observed for SNR≤2. Additionally, variability in forecast skill appears to be higher for low SNR values. The threshold SNR = 2 roughly corresponds to the value where the elbow in Fig. 8b and e is located.

Plots in Fig. 9 show the frequency distribution of MAD values between the forecast and the reanalysis of dry extremes (SSI < -0.67) for different classes of SNR: low (< 2) and high (> 2). Results indicate that, on average, smaller average differences are observed for high SNR values (> 2) compared to low SNR values (< 2). Additionally, the results are less spread around the mean for SNR > 2 compared to the low SNR case, where the frequency distribution is rather flat. This difference is particularly true for SSI-3 DJF (Fig. 9b).

4 Discussion

This study provides an overall assessment of the skill of CEMS seasonal forecast of river discharge for the detection of hydrological droughts at three accumulation periods (1, 3, and 6 months) globally. Our results show generally high skill in predicting hydrological drought conditions in terms of correlation between the esemble mean forecast forced by

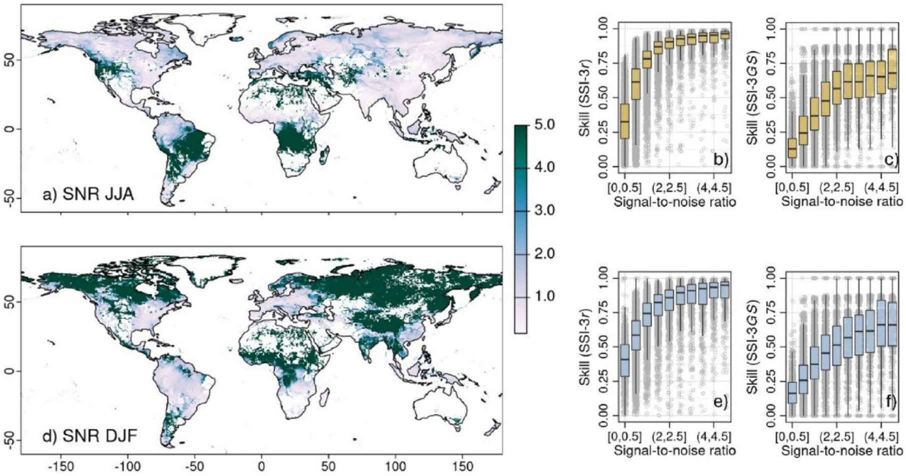

Fig. 8 Time-averaged SNR, and scatterplots of the relation between the Pearson *r* (SSI-3*r*) and SNR and the Gilbert Skill Score (SSI-3*GS*) and SNR for **a**–**c** summer (JJA) and **d**–**f** winter (DJF). Pearson *r* ranges from −1 to 1, and GS ranges from −1/3 to 1. Similarly to the other figures, as no negative values were estimated, the ranges are set to 0–1

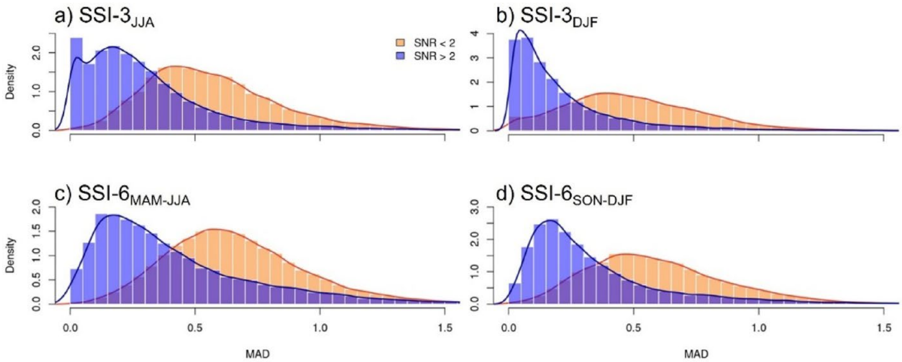

Fig. 9 Density histograms of the Mean absolute difference (MAD) between ensemble mean forecast and reanalysis for SSI-3, **a** summer, JJA, and **b** winter, DJF, and SSI-6, **c** spring–summer, MAM-JJA, and **d** autumn–winter, SON-DJF for SNR > 2 (in purple) and SNR < 2 (in light orange)

SEAS5 model and the ERA5 reanalysis, well beyond what is commonly obtained on meteorological droughts (e.g., Lavaysse et al. 2015). This result is in general agreement with the conclusions of previous studies performed at the European scale, e.g., by Sutanto et al. (2020). Higher forecast skill is generally found in northwest Northern America and the southernmost areas of South America (e.g., Paraná River Basin), the Congo River Basin in Central Africa, some regions in Northern and Eastern Europe, and Eastern Asia (Fig. 2a). Overall, good streamflow forecast skill in Europe was observed over the entire domain by Pechlivanidis et al. (2020) at lead time 0, although with geographical and seasonal variability. In contrast, East of the US, Western Africa, Southern and Central Europe, India, North Korea, and the Republic of Korea and Japan show lower skill at the 6-month time scale

(Fig. 2a). In general, beyond 3 months the forecast skill declines as also observed in Lee et al. (2024), especially during wet years, across catchments in the Republic of Korea.

We also find different skill patterns depending on the season. A sharp contrast exists, for example, in India and Eastern Asia, with significant skill in winter (DJF), when river discharge appears predictable for up to three months, and low to no skill for summer (JJA). Chevuturi et al. (2021) also pointed out the overall underestimation of the Indian Summer Monsoon rainfall over the Indian subcontinent in, but not limited to, the ECMWF SEAS5 forecasting system. Still, they found that SEAS5 has good skill at predicting large-scale monsoon features, but it has less skill for smaller-scale indices. Another area exhibiting important differences is the Amazon basin, which, in contrast, has higher skill in JJA than DJF. Over Europe, our results pointing to higher predictability in spring and summer are in agreement with Pechlivanidis et al. (2020). The improved forecast capability on drought events during low average river discharge values can have important practical consequences. Usually, droughts are more impactful during climatologically lower (on average) phases of river discharge, as the general lack of water is further exacerbated by the drought. In this context, the observed differences in skill across seasons are encouraging for operational applications, as the drought conditions occurring during the seasons with low average river discharge seem to be better predicted.

The comparison of the forecast performance against the trivial forecast using the last previously available reanalysis data explores the potential added value of the hydrological drought seasonal forecast compared to a system based only on monitoring. The accuracy of the seasonal forecast outperforms persistence over most of the study domain with an outbreak for 3 and 6 months ahead for Northern latitudes (over 50° N) in spring–summer (MAM-JJA) (Fig. 5d–f). As noticed by Yossef et al. (2013) in this season, even for a month accumulation period, the predictability of the forecast is dominated by the meteorological forcings, coinciding with the snow and ice melting process. Nevertheless, there are areas where the added value is less marked, such as those in the Tropical region for SSI-3 and SSI-6 in MAM-JJA.

The quality of the seasonal river discharge forecast depends on the correct estimation of the initial conditions and on the quality of meteorological forcings predictions. Results here show that if the initial conditions have a lower inter-annual variability, higher forecast skill is mostly driven by how well the meteorological forcings are forecasted (and less on the initial conditions) (e.g., Fig. 6a). The results show that getting the initial conditions right can enhance the hydrological drought forecast skill, although mean differences remain limited compared to data spread and additional investigation is needed to confirm the pattern. Across different scales, studies such as Wood and Lettenmaier (2008), Yossef et al. (2013) and Greuell and Hutjes (2023) found that the relative importance of one or another driver changes seasonally and with lead time, highlighting the need to target the dominant source of uncertainty, either through improved initial condition estimates, by data assimilation of satellite and/or micro-sensor data, or improved weather forecasts.

The SNR is evaluated to globally complement the analysis of predictability. Overall, ensemble-mean forecast skill increases with higher SNR values in both summer (JJA) and winter (DJF) (Fig. 8b and e), highlighting SNR as a valuable intrinsic measure of predictability for hydrological drought forecasts. These results are consistent with Acosta Navarro and Toreti (2023), who pointed out the relevance of years with extreme SNR values on obtained skillful summer (JJA) air temperature and precipitation forecasts. They also identified several cases in the Northern Hemisphere where low SNR corresponds to minimal anomaly differences, particularly in regions lacking predictive skill. Additionally, Doi et al. (2022) highlighted the importance of sampling years with the highest SNR for improving forecast accuracy. Communicating near real-time forecast reliability is critical to addressing user-relevant needs and, consistently with current best practices of operational verification, supports transparency and enhances trust. In addition, routinely monitoring forecast performance and alerting stakeholders when it deteriorates is fundamental to maintaining that confidence (Pagano et al. 2025).

Notwithstanding, our results also show a clear distinction in the frequency of absolute difference between ensemble-mean forecasts and reanalysis according to the SNR, supporting the common understanding that high-coherent ensembles (high SNR) tend to be more skillful. Since the availability of skillful hydrological drought forecasts is of utmost importance for stakeholders' early decision-making, further work on ensemble member selection may enhance ensemble coherence, impacting forecast predictability.

5 Summary and conclusions

Drought is considered one of the most extreme natural hazards. Prolonged meteorological drought conditions propagate into agricultural and hydrological droughts, which are the levels at which damages are observed and reported. It follows that the availability of hydrological drought forecasts represents an opportunity to develop early warning systems and contingency plans based on a proactive approach. Herein, we assessed the use of seasonal river discharge forecasts from CEMS GloFAS to predict hydrological drought conditions. We found that the predictability of the SSI for the period 1991–2022 remains high even at the 6-month time horizon (average Pearson $r > 0.6$), even if it understandably drops compared to a month time horizon (Pearson $r = 0.81 \pm 0.11$). It is worth noting that the skill is evaluated against a reanalysis (ERA5), so further analyses using observations may be useful. Despite this limitation, results are promising, characterized by clear spatial patterns, with some regions (e.g., the Congo River Basin or Southern South America) retaining good skill even at a 6-month forecast horizon (Pearson $r > 0.8$). The spatiotemporal dependence of skill becomes apparent when results are compared to river seasonality, as we found higher skill with lower average river discharge. In addition, a key role of the inter-annual variability in initial conditions and meteorological forcings on forecast skill is observed, with the former impacting especially summer (JJA) and spring–summer (MAM-JJA) forecasts and the latter influencing winter (DJF) and autumn–winter (SON-DJF) forecasts.

In the framework of an operational implementation of a drought forecast system based on SSI, the results show a net overall improvement over the latest available reanalysis data, suggesting added value in support of decision making. This is especially true in Northern latitudes during MAM-JJA and for 3 and 6 months ahead, as the memory effect is limited. Finally, auxiliary information on the reliability of the forecast can be inferred directly from measurements of ensemble spread, such as the SNR. The obtained results recommend the inclusion of this quantity, alongside the ensemble-mean, to highlight forecasts characterized by high reliability (SNR > 2 in this study).

Supplementary Information The online version contains supplementary material available at https://doi.org/10.1007/s11069-025-07751-w.

Acknowledgements This study has been supported by the Horizon Europe project SEED-FD (Strengthening Extreme Events Detection for Flood and Drought) HORIZON-CL4-2023-SPACE-01-32 (CUP: D43C23003660006-2023).

Author contributions V. García-Gamero: Formal analysis, Investigation, Methodology, Software, Visualization, Writing—original draft, Writing—review & editing. C. Cammalleri: Conceptualization, Data curation, Methodology, Supervision, Validation, Visualization, Writing—original draft, Writing—review & editing. A. Ceppi: Data curation, Formal analysis, Writing—review & editing. C. Prudhomme: Data curation, Formal analysis, Writing—review & editing. A. Ramos: Data curation, Formal analysis, Writing—review & editing. J.C. Acosta Navarro: Conceptualization, Methodology, Writing—review & editing. A. Toreti: Conceptualization, Methodology, Writing—review & editing.

Funding Horizon Europe project SEED-FD (Strengthening Extreme Events Detection for Flood and Drought) HORIZON-CL4-2023-SPACE-01-32 (CUP: D43C23003660006-2023).

Declarations

Conflict of interest The authors have no relevant financial or non-financial interests to disclose.

References

Acosta Navarro JC, Toreti A (2023) Exploiting the signal-to-noise ratio in multi-system predictions of boreal summer precipitation and temperature. Weather Clim Dynam 4:823–831. https://doi.org/10.5194/wcd-4-823-2023

Aghakouchak A, Pan B, Mazdiyasni O, Sadegh M, Jiwa S, Zhang W, Love CA, Madadgar S, Papalexiou SM, Davis SJ, Hsu K, Sorooshian S (2022) Status and prospects for drought forecasting: opportunities in artificial intelligence and hybrid physical-statistical forecasting. Phil Trans R Soc A 380:20210288. https://doi.org/10.1098/rsta.2021.0288

Arias PA, Rivera JA, Sörensson AA, Zachariah M, Barnes C, Philip S, Kew S, Vautard R, Koren G, Pinto I, Vahlberg M, Singh R, Raju E, Li S, Yang W, Vecchi GA, Otto FEL (2024) Interplay between climate change and climate variability: the 2022 drought in Central South America. Clim Change 177:6. https://doi.org/10.1007/s10584-023-03664-4

Arora VK, Harrison S (2007) Upscaling river networks for use in climate models. Geophys Res Lett 34:L21407. https://doi.org/10.1029/2007GL031865

Biella R, Shyrokaya A, Ionita M et al (2025) The 2022 drought needs to be a turning point for European drought risk management. Nat Hazards Earth Syst Sci 25:4475–4501. https://doi.org/10.5194/nhess-25-4475-2025

Bierkens MFP, Van Beek LPH (2009) Seasonal predictability of European discharge: NAO and hydrological response time. J Hydrometeorol 10(4):953–968. https://doi.org/10.1175/2009JHM1034.1

Cammalleri C, Naumann G, Mentaschi L, Bisselink B, Gelati E, De Roo Ad, Feyen L (2020) Diverging hydrological drought traits over Europe with global warming. Hydrol Earth Syst Sci 24:5919–5935. https://doi.org/10.5194/hess-24-5919-2020

Chevuturi A, Turner AG, Johnson S, Weisheimer A, Shonk JKP, Stockdale TN, Senan R (2021) Forecast skill of the Indian monsoon and its onset in the ECMWF seasonal forecasting system 5 (SEAS5). Clim Dyn 56(9–10):2941–2957. https://doi.org/10.1007/s00382-020-05624-5

European Commission (2025) Indicator for forecasting unusually wet and dry conditions (Joint Research Centre, Ed.). Copernicus European drought observatory.

Dasgupta A, Arnal L, Emerton R et al (2025) Connecting hydrological modelling and forecasting from global to local scales: perspectives from an international joint virtual workshop. J Flood Risk Manag 18(1):e12880. https://doi.org/10.1111/JFR3.12880

Day GN (1985) Extended streamflow forecasting using nwsrfs. J Water Resour Plan Manag 111:157–170. https://doi.org/10.1061/(ASCE)0733-9496(1985)111:2(157)

De Roo APJ, Wesseling CG, Van Deursen WPA (2000) Physically based river basin modelling within a GIS: the LISFLOOD model. Hydrol Process 14(11–12):1981–1992. https://doi.org/10.1002/1099-1085(20000815/30)14:11/12%3c1981::aid-hyp49%3e3.0.co;2-f

Doi T, Nonaka M, Behera S (2022) Can signal-to-noise ratio indicate prediction skill? Based on skill assessment of 1-month lead prediction of monthly temperature anomaly over Japan. Front Clim 4:887782. https://doi.org/10.3389/fclim.2022.887782

Emerton R, Zsoter E, Arnal L, Cloke HL, Muraro D, Prudhomme C, Stephens EM, Salamon P, Pappenberger F (2018) Developing a global operational seasonal hydro-meteorological forecasting system: GloFAS-Seasonal v1.0. Geosci Model Dev 11(8):3327–3346. https://doi.org/10.5194/gmd-11-3327-2018

Forzieri G, Feyen L, Rojas R, Flörke M, Wimmer F, Bianchi A (2014) Ensemble projections of future streamflow droughts in Europe. Hydrol Earth Syst Sci 18:85–108. https://doi.org/10.5194/hess-18-85-2014

Greuell W, Hutjes RWA (2023) Skill and sources of skill in seasonal streamflow hindcasts for South America made with ECMWF's SEAS5 and VIC. J Hydrol 617:128806. https://doi.org/10.1016/j.jhydrol.2022.128806

Grimaldi S, Salamon P, Disperati J, Zsoter E, Russo C, Ramos A, Carton De Wiart C, Barnard C, Hansford E, Gomes G, Prudhomme C (2022) River discharge and related historical data from the global flood awareness system, v4.0. European commission, joint research centre (JRC). https://doi.org/10.24381/cds.a4fdd6b9 (Accessed on 18-07-2025)

Grimaldi S, Salamon P, Disperati J, Zsoter E, Russo C, Ramos A, Carton De Wiart C, Barnard C, Hansford E, Gomes G, Prudhomme C (2023) Seasonal reforecasts of river discharge and related data by the global flood awareness system, v4.0. European Commission, joint research centre (JRC). https://doi.org/10.24381/cds.0aa9b9dd (Accessed on 18-07-2025)

Hao Z, Singh VP, Xia Y (2018) Seasonal drought prediction: advances, challenges, and future prospects. Rev Geophys 56(1):108–141. https://doi.org/10.1002/2016RG000549

Harrigan S, Zsoter E, Alfieri L, Prudhomme C, Salamon P, Wetterhall F, Barnard C, Cloke H, Pappenberger F (2020) GloFAS-ERA5 operational global river discharge reanalysis 1979-present. Earth Syst Sci Data 12(3):2043–2060. https://doi.org/10.5194/essd-12-2043-2020

Hersbach H, Bell B, Berrisford P, Hirahara S, Horányi A, Muñoz-Sabater J, Nicolas J, Peubey C, Radu R, Schepers D, Simmons A, Soci C, Abdalla S, Abellan X, Balsamo G, Bechtold P, Biavati G, Bidlot J, Bonavita M, Thépaut JN (2020) The ERA5 global reanalysis. Q J R Meteorol Soc 146(730):1999–2049. https://doi.org/10.1002/qj.3803

Hoerling M, Eischeid J, Kumar A, Leung R, Mariotti A, Mo K, Schubert S, Seager R (2014) Causes and predictability of the 2012 great plains drought. Bull Amer Meteorol Soc 95(2):269–282. https://doi.org/10.1175/BAMS-D-13-00055.1

Johnson SJ, Stockdale TN, Ferranti L, Balmaseda MA, Molteni F, Magnusson L, Tietsche S, Decremer D, Weisheimer A, Balsamo G, Keeley SPE, Mogensen K, Zuo H, Monge-Sanz BM (2019) SEAS5: the new ECMWF seasonal forecast system. Geosci Model Dev 12:1087–1117. https://doi.org/10.5194/gmd-12-1087-2019

Jolliffe IT, Stephenson DB (eds) (2003) Forecast verification. Wiley, New York

Lackstrom K, Farris A, Eckhardt D, Doesken N, Reges H, Turner J, Smith KH, Ward R (2017) CoCoRaHS observers contribute to "condition monitoring" in the Carolinas: a new initiative addresses needs for drought impacts information. Bull Amer Meteorol Soc 98(12):2527–2531. https://doi.org/10.1175/BAMS-D-16-0306.1

Lavaysse C, Vogt J, Pappenberger F (2015) Early warning of drought in Europe using the monthly ensemble system from ECMWF. Hydrol Earth Syst Sci 19:3273–3286. https://doi.org/10.5194/hess-19-3273-2015

Lavaysse C, Mccormick N, Vogt J (2020) Evaluation of a new precipitation-based index for global seasonal forecasting of unusually wet and dry periods. Weather Forecast 35:1189–1202. https://doi.org/10.1175/WAF-D-19-0196.1

Lee Y, Pianosi F, Peñuela A, Rico-Ramirez MA (2024) Skill of seasonal flow forecasts at catchment scale: an assessment across South Korea. Hydrol Earth Syst Sci 28:3261–3279. https://doi.org/10.5194/hess-28-3261-2024

Mckee TB, Doesken NJ, Kleist J (1993) The relationship of drought frequency and duration to time scales. In: Eighth conference on applied climatology, 17–22.

Merryfield WJ, Baehr J, Batté L, Becker EJ, Butler AH, Coelho CAS, Danabasoglu G, Dirmeyer PA, Doblas-Reyes FJ, Domeisen DIV, Ferranti L, Ilynia T, Kumar A, Müller WA, Rixen M, Robertson AW, Smith DM, Takaya Y, Tuma M, Vitart F, White CJ, Alvarez MS, Ardilouze C, Attard H, Baggett C, Balmaseda MA, Beraki AF, Bhattacharjee PS, Bilbao R, de Andra FM, DeFlorio MJ, Díaz LB, Ehsan MA, Fragkoulidis G, Gonzalez AO, Grainger S, Green BW, Hell MC, Infanti JM, Isensee K, Kataoka T, Kirtman BP, Klingaman NP, Lee J-Y, Mayer K, McKay R, Mecking JV, Miller DE, Neddermann N, Justin Ng CH, Ossó A, Pankatz K, Peatman S, Pegion K, Perlwitz J, Recalde-Coronel GC, Reintges A, Renkl C, Solaraju-Murali B, Spring A, Stan C, Sun YQ, Tozer CR, Vigaud N, Woolnough S, Yeager S (2020) Current and emerging developments in subseasonal to decadal prediction. Bull Am Meteorol Soc 101(6):E869–E896. https://doi.org/10.1175/BAMS-D-19-0037.1

Mishra V, Thirumalai K, Jain S, Aadhar S (2021) Unprecedented drought in South India and recent water scarcity. Environ Res Lett 16(5):054007. https://doi.org/10.1088/1748-9326/abf289

Nicolai-Shaw N, Gudmundsson L, Hirschi M, Seneviratne SI (2016) Long-term predictability of soil moisture dynamics at the global scale: persistence versus large-scale drivers. Geophys Res Lett 43(16):8554–8562. https://doi.org/10.1002/2016GL069847

Pagano TC, Ebert EE, Khanarmuei M (2025) Enhancing forecast verification in national meteorological and hydrological services. Meteorol Appl 32:e70051. https://doi.org/10.1002/MET.70051

Pechlivanidis IG, Crochemore L, Rosberg J, Bosshard T (2020) What are the key drivers controlling the quality of seasonal streamflow forecasts? Water Resour Res 56(6):e2019WR026987. https://doi.org/10.1029/2019WR026987

Rebetez M, Mayer H, Dupont O, Schindler D, Gartner K, Kropp JP, Menzel A (2006) Heat and drought 2003 in Europe: a climate synthesis. Ann for Sci 63(6):569–577. https://doi.org/10.1051/forest:2006043

Sepulcre-Canto G, Horion S, Singleton A, Carrao H, Vogt J (2012) Natural Hazards and Earth system sciences development of a combined drought indicator to detect agricultural drought in Europe. Hazards Earth Syst Sci 12:3519–3531. https://doi.org/10.5194/nhess-12-3519-2012

Shao Q, Li M (2013) An improved statistical analogue downscaling procedure for seasonal precipitation forecast. Stoch Environ Res Risk Assess 27(4):819–830. https://doi.org/10.1007/s00477-012-0610-0

Shi X, Wood AW, Lettenmaier DP (2008) How essential is hydrologic model calibration to seasonal stream flow forecasting? J Hydrometeorol 9(6):1350–1363. https://doi.org/10.1175/2008JHM1001.1

Shukla S, Sheffield J, Wood EF, Lettenmaier DP (2013) On the sources of global land surface hydrologic predictability. Hydrol Earth Syst Sci 17(7):2781–2796. https://doi.org/10.5194/hess-17-2781-2013

Sousa PM, Blamey RC, Reason CJC, Ramos AM, Trigo RM (2018) The "Day Zero" Cape Town drought and the poleward migration of moisture corridors. Environ Res Lett 13(12):124025. https://doi.org/10.1088/1748-9326/aaebc7

Stahl K, Kohn I, Blauhut V, Urquijo J, De Stefano L, Acácio V, Dias S, Stagge JH, Tallaksen LM, Kampragou E, Van Loon AF, Barker LJ, Melsen LA, Bifulco C, Musolino D, De Carli A, Massarutto A, Assimacopoulos D, Van Lanen HAJ (2016) Impacts of European drought events: insights from an international database of text-based reports. Nat Hazards Earth Syst Sci 16(3):801–819. https://doi.org/10.5194/nhess-16-801-2016

Sutanto SJ, Van Lanen HAJ (2021) Streamflow drought: implication of drought definitions and its application for drought forecasting. Hydrol Earth Syst Sci 25:3991–4023. https://doi.org/10.5194/HESS-25-3991-2021

Sutanto SJ, Wetterhall F, Van Lanen HAJ (2020) Hydrological drought forecasts outperform meteorological drought forecasts. Environ Res Lett 15(8):084010. https://doi.org/10.1088/1748-9326/ab8b13

Sutanto SJ, Syaehuddin WA, de Graaf I (2024) Hydrological drought forecasts using precipitation data depend on catchment properties and human activities. Commun Earth Environ 5:118. https://doi.org/10.1038/s43247-024-01295-w

Tallaksen LM, van Lanen HAJ (Eds.; Second) (2023) Hydrological drought: processes and estimation methods for streamflow and groundwater. Elsevier. https://doi.org/10.1016/C2017-0-03464-X

Thober S, Kumar R, Sheffield J, Mai J, Schäfer D, Samaniego L (2015) Seasonal soil moisture drought prediction over Europe using the North American multi-model ensemble (NMME). J Hydrometeorol 16(6):2329–2344. https://doi.org/10.1175/JHM-D-15-0053.1

Toreti A, Belward A, Perez-Dominguez I, Naumann G, Luterbacher J, Cronie O, Seguini L, Manfron G, Lopez-Lozano R, Baruth B, van den Berg M, Dentener CA, Chatzopoulos T, Zampieri M (2019) The exceptional 2018 European water seesaw calls for action on adaptation. Earths Future 7(6):652–663. https://doi.org/10.1029/2019EF001170

Troin M, Arsenault R, Wood AW, Brisette F, Martel JL (2021) Generating ensemble streamflow forecasts: A review of methods and approaches over the past 40 years. Water Resour Res 57:e2020WR028392. https://doi.org/10.1029/2020WR028392

United Nations Office for Disaster Risk Reduction (UNDRR) (2021) GAR special report on drought 2021. Geneva.

United Nations Office for Disaster Risk Reduction (UNDRR) (2022) Global assessment report on disaster risk reduction 2022: Our world at risk: Transforming governance for a resilient future. Geneva.
Van der Knijff JM, Younis J, De Roo APJ (2010) LISFLOOD: a GIS-based distributed model for river basin scale water balance and flood simulation. Int J Geogr Inf Sci 24(2):189–212. https://doi.org/10.1080/13658810802549154
Van Dijk AI, Beck HE, Crosbie RS, De Jeu RA, Liu YY, Podger GM, Timbal B, Viney NR (2013) The millennium drought in southeast Australia (2001–2009): natural and human causes and implications for water resources, ecosystems, economy, and society. Water Resour Res 49(2):1040–1057. https://doi.org/10.1002/wrcr.20123
Viste E, Korecha D, Sorteberg A (2013) Recent drought and precipitation tendencies in Ethiopia. Theor Appl Climatol 112(3–4):535–551. https://doi.org/10.1007/s00704-012-0746-3
Wilks DS (2020) Statistical methods in the atmospheric sciences (Fourth). Elsevier, Amsterdam
Wood AW, Lettenmaier DP (2008) An ensemble approach for attribution of hydrologic prediction uncertainty. Geophys Res Lett. https://doi.org/10.1029/2008GL034648
Wood EF, Schubert SD, Wood AW, Peters-Lidard CD, Mo KC, Mariotti A, Pulwarty RS (2015) Prospects for advancing drought understanding, monitoring, and prediction. J Hydrometeorol 16(4):1636–1657. https://doi.org/10.1175/JHM-D-14-0164.1
World Meteorological Organization (WMO) (2017) Guidelines on the calculation of climate normals (WMO-No.1203).
World Meteorological Organization (WMO), Global Water Partnership (GWP) (2016) Handbook of drought indicators and indices (M. Svoboda and B.A. Fuchs). Integrated Drought Management Programme (IDMP), Integrated Drought Management Tools and Guidelines Series 2. Geneva
Yossef NC, Winsemius H, Weerts A, Van Beek R, Bierkens MFP (2013) Skill of a global seasonal streamflow forecasting system, relative roles of initial conditions and meteorological forcing. Water Resour Res 49(8):4687–4699. https://doi.org/10.1002/wrcr.20350
Yuan X, Wood EF, Chaney NW, Sheffield J, Kam J, LiangM G (2013) Probabilistic seasonal forecasting of African drought by dynamical models. J Hydrometeorol 14(6):1706–1720. https://doi.org/10.1175/JHM-D-13-054.1
Zhang X, Tang Q, Liu X, Leng G, Li Z (2017) Soil moisture drought monitoring and forecasting using satellite and climate model data over southwestern China. J Hydrometeorol 18(1):5–23. https://doi.org/10.1175/JHM-D-16-0045.1

Authors and Affiliations

Vanesa García-Gamero[1] · Carmelo Cammalleri[1] · Alessandro Ceppi[1] · Christel Prudhomme[2] · Arthur Ramos[2] · Juan Camilo Acosta Navarro[3] · Andrea Toreti[3]

✉ Vanesa García-Gamero
vanesa.garcia@polimi.it

1 Politecnico di Milano, Dipartimento di Ingegneria Civile e Ambientale (DICA), Milan, Italy

2 European Centre for Medium-Range Weather Forecasts (ECMWF), Reading, UK

3 European Commission, Joint Research Centre, Ispra, Italy